JARQ 55 (2), 177-190 (2021) https://www.jircas.go.jp

Long-term Hydrological Observations in a Lowland Dry Evergreen Forest Catchment Area of the Lower Mekong River, Cambodia

Naoki KABEYA[1]*, Akira SHIMIZU[1], Takanori SHIMIZU[2], Shin'ichi IIDA[2], Koji TAMAI[2], Asako MIYAMOTO[2], Sophal CHANN[3], Makoto ARAKI[2] and Yasuhiro OHNUKI[4]

[1] Kyushu Research Centre, Forestry and Forest Products Research Institute, Kumamoto, Japan
[2] Forestry and Forest Products Research Institute, Tsukuba, Japan
[3] Forest and Wildlife Science Research Institute, Forestry Administration, Phnom Penh, Cambodia
[4] Tohoku Research Centre, Forestry and Forest Products Research Institute, Morioka, Japan

Abstract

Long-term field observation was clarified over ten years for the water budget of Cambodia's forest watershed, one of the world's most data-sparce areas. The La Niña years had large amounts of annual rainfall exceeding 1,800 mm, often marked by monsoon breaks during the rainy season. The El Niño years had smaller amounts of annual rainfall between 1,100 mm and 1,200 mm, aside from that in 2016. The strong El Niño during 2015-2016 caused large drops in both river and groundwater levels in the Cambodian forest catchment. However, the former levels of groundwater and river water were restored by 953.4 mm of rain received during the second half of the rainy season in 2016. Thus, the monsoon breaks may be correlated with the increased amount of rainfall in the second half of the rainy season.

Discipline: Forestry
Additional key words: El Niño-Southern Oscillation, monsoon break, water balance

Introduction

Cambodia is part of the Southeastern Indochina ecoregion that includes Vietnam, Laos, Thailand, and Myanmar (Wikramanayaka et al. 2002). The evergreen broadleaf forest in the Cambodian central plain is situated at low altitudes and latitude (19-653 m ASL, latitude 12° 44′N, respectively), and has mean annual precipitation of 1,500 mm-1,800 mm (Kabeya et al. 2007, Save Cambodia's Wildlife (SCW) 2006). According to Ashton (1991), this forest is classified as "dry evergreen" due to water stress from a dry season lasting for at least five months. The northern edge of this forest is in the northern parts of Thailand and Myanmar, where human impact is creating changes in land use (Ashton 1991). This type of forest remains widely distributed in Cambodia in the Indochinese Peninsula of the lower Mekong river basin (Asian Development Bank (ADB) - The United Nations Environment Programme (UNEP) 2004), but development is quickly increasing across the peninsula. Therefore, it is important to understand the hydrological processes within the lowland, dry, evergreen forest watershed in Cambodia, in order to understand the water cycle of the terrestrial ecosystem in the Indochinese Peninsula.

The Asian summer monsoon is a major feature of the general circulation that dominates East Asia for more than a third of the year, and it influences many remote regions. The monsoon exhibits substantial interannual variability, which has profound social and economic consequences (Callaghan & Bonell 2005). This variability is closely related to the El Niño/Southern Oscillation (ENSO) (e.g., Rasmusson & Carpenter 1983, Webster & Yang 1992), where years in an El Niño phase have a weaker monsoon circulation with a delayed onset, whereas the La Niña phase coincides with the opposite behavior (Ju & Slingo 1995, Zhang et al. 2002). The ENSO is the primary driver of temperature variation across the tropics and rainfall fluctuations over a large area of Southeast Asia (Malhi & Wright 2004) on an

*Corresponding author: kabeya@affrc.go.jp
Received 6 March 2020; accepted 9 September 2020.

interannual scale. Most ENSO studies to date have focused on the relationship with rainfall levels. Therefore, the effects of interannual variability of rainfall associated with the ENSO on the hydrological processes within a forest catchment area are still not understood well. Cambodia has a subtropical climate governed by two monsoon seasons: the cool, dry northeastern monsoon from November to March, and the humid southwestern monsoon from May to October. In the inland region of the Indochina Peninsula, the rainy season usually begins in late April to early May and then weakens in mid-October to mid-November (Matsumoto 1997). The onset of the rainy season is earlier in the inland region than around the coast near the Bay of Bengal; such an early onset occurs due to different wind behavior at mid-latitudes, and can thus be considered ‘‘pre-monsoon rain” (Matsumoto 1997). Some pre-monsoon rain was observed from March to April at our study sites (Kabeya et al. 2007). To date, there are no published observations of watershed on basin water balance in lowland evergreen forests during the dry season that are also in a strong El Niño phase, which may cause severe drought and lower available water resources in this area. Yoshifuji et al. (2007) studied the interannual variability of evapotranspiration during the rainy and growing seasons for artificially planted teak trees in Thailand. Similar studies have never been conducted for natural dry evergreen forests.

In order to investigate the water cycle in lowland dry forests, the Evergreen Forest Experimental Watershed was established in the Stung Chinit river basin in Kampong Thom, Cambodia (Shimizu et al. 2007). This watershed consists of four catchments, with drainage areas ranging from 4 km^2 to 3,659 km^2. The experimental forest watershed has an integrated hydrological observation system that includes a 60-m-high meteorological observation tower for the examination of forest evapotranspiration. Kabeya et al. (2008) have reported preliminary research results that focused on year-round variations. Thus, we aimed to clarify long-term field observation over ten years (2007 to 2016) for the water budget of Cambodia's forest watershed, one of the world's most data-sparce areas. This 10-year observation period includes both heavy rainfall and drought events associated with the ENSO. In particular, a strong El Niño (named super El Niño) event occurred during the observation period from 2015 to 2016, and its effect on the forest watershed was also evaluated.

Study site and methods

1. Study site

The Evergreen Forest Experimental Watershed of the Stung Chinit River is located in Kampong Thom, Cambodia. The Stung Chinit River runs through the Cambodian Central Plain into Tonle Sap Lake, marked by many evergreen broadleaf forests. Figure 1 shows the runoff observation point for the Stung Chinit catchment (CT), which has a drainage area of 3,659 km^2. Although the altitude ranges from 19 m to 653 m, 90% of the drainage area is below 140 m; thus, the watershed has very flat topography (as per the digital elevation model based on Forestry Administration, Cambodia 50 m × 50 m topographical database, Kabeya et al. 2008). There is a meteorological tower located in the headwaters area of the O Thom I catchment. Further details regarding these sub-catchments can be found in Kabeya et al. (2008).

The surface geology is of the quaternary period and consists of a river terrace overlaid with sedimentary rocks (Ohnuki et al. 2007). The soil type changes with the type of vegetation: haplic acrisols (Food and Agriculture Organization (FAO) - United Nations Educational, Scientific and Cultural Organization (UNESCO) Classification) are found under the evergreen broadleaf forest, the dominant vegetation type of this area (Toriyama et al. 2007). The acrisol-alisol group occurs widely throughout Southeast Asia, including the Mekong River basin and particularly in Cambodia, where quaternary sediments exist (Chappell et al. 2007). Soil thickness in the dry evergreen forest in this area is over 8 m, and the effective porosity of the soil is 0.13 m^3 m^{-3} (Ohnuki et al. 2008). For the same study site, the saturated hydraulic conductivity was between 2.0×10^{-5} m s^{-1} to 3.0×10^{-6} m s^{-1} from the surface to a depth of 60 cm (Shinomiya et al. 2007).

The observation study site is a dry evergreen forest in which *Myristica iners*, *Dipterocarpus costatus*, *Anisoptera costata*, and *Vatica odorata* are the major species (Ito et al. 2007). The largest tree at the tower site is 45-m tall, with a diameter at breast height (DBH) of 1.2 m (Shimizu et al. 2007), and a leaf area index (LAI) of 4.0 m^2 m^{-2} (Ito et al. 2007). Nobuhiro et al. (2007) made evapotranspiration measurements at a dry evergreen forest tower site in Kampong Thom, Cambodia, from November 2003 to October 2004, using the Bowen ratio method. They found that evapotranspiration was approximately 4.0 mm day^{-1} throughout the dry season, and approximately 2.0 mm day^{-1} in the rainy season. The tree roots extend to a depth of 8 m-9 m, and the forest maintains active evapotranspiration during the dry season using water stored in this deep soil layer

(Nobuhiro et al. 2007, Toriyama et al. 2013).

2. Land use change

Figure 2 shows land use in the Stung Chinit watershed in 2002 and 2014. The Japan International Cooperation Agency (JICA) provided the data for 2002 in 2003, but the data can also be found in Kabeya et al. (2008). Cambodia's Forest Administration provided the data for 2014. Note that the land use classification changed between 2002 and 2014. In Kabeya et al. (2008), the mixed forest was considered its own class, but a field survey showed that deciduous trees dominated mixed forests. Thus, this study combined the two. Moreover, the marginal area of a rubber plantation was added to the field crop classification in 2002. However, the area of the rubber plantation vastly increased in 2014; thus, this

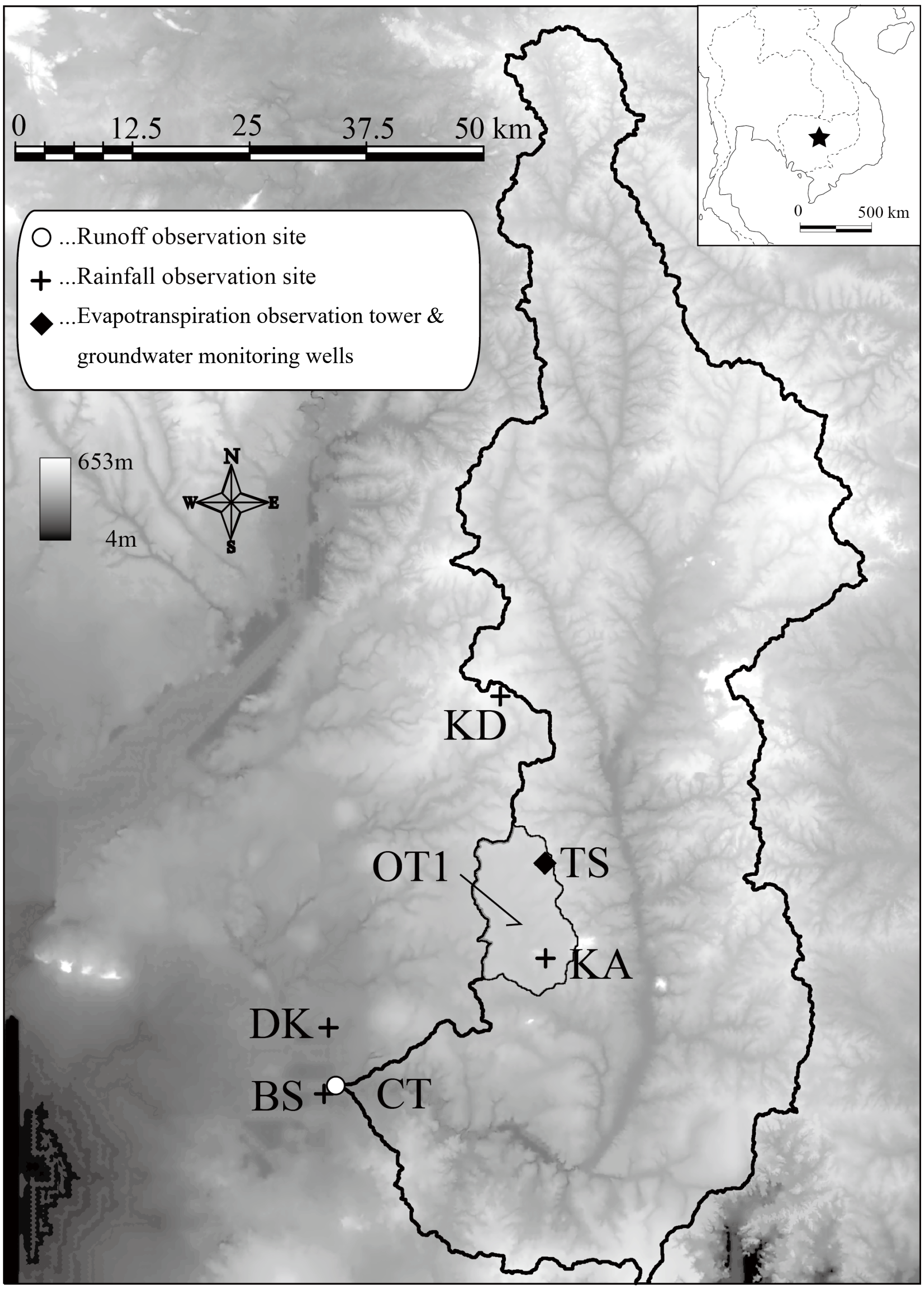

Fig. 1. The Evergreen Forest Experimental Watershed of the Stung Chinit (CT) River, Kampong Thom Province, Cambodia

Rainfall was observed at Bak Snar (BS), Dong Kda (DK), Kamb Ambel (KA), and Kbal Domrey (KD). Runoff from the Stung Chinit watershed was observed at CT. Groundwater level was observed at the Tower Site (TS) in the headwaters part of the O Thom I (OT1) sub-catchment.

study again classifies such areas into their own classification.

The percentage of forested area in the evergreen experimental watershed (including evergreen broadleaf, deciduous, and bamboo/secondary forests in three watersheds) was 89% in 2002. This value was reduced to 61% by 2014. Between 2002 and 2014, the deciduous forests decreased by 20%. By 2014, evergreen forests decreased by 4% overall, but still accounted for the main land use at 55%. Shrubland and grassland also decreased by 2%. While the percentage of deciduous forests decreased, the land use for field crops and rubber plantations increased by 24% and 6%, respectively.

3. Observation method

(1) River water observation and runoff calculation

Figure 1 shows the river water level observation point in Stung Chinit. Between the bank ridges, the river stretches 23.6 m in width and 11.4 m in depth from the bank ridges to the riverbed. This information was based on a cross-sectional survey conducted on 21 February 2003. The Asian Development Bank (ADB) built the Stung Chinit River irrigation dam in 2005; the dam stands 6-m tall and is located 27 km from the water-level observation point of CT (ADB 2012). The water stored in the resulting reservoir is used to automatically irrigate the surrounding paddy fields, utilizing a system based on gravity. Following construction of the dam, the river water level at CT during dry periods increased to 6 m in 2006, which also changed the river flow velocity. River flow velocity was measured using by floating buoys more than 10 times between 2007 and 2016, and rating curves were re-created based on the observations in the following equation:

$$D = 16.687\,(H - 5.0)^2 \quad [6 < H] \qquad (1)$$

where D is the discharge (m^3/s) and H is the water level (m). Flow velocity data were only calculated by Eq. (1) when the water level at CT was between 6 m and 11.4 m because for 6 m or less, the river almost changed into a stagnant water condition, thus making the measurement of flow velocity difficult. When H was 6 m or less, D was set as zero.

The river water level was recorded daily at 0900 and 1600 from a manual measurement using a buzzer-type level gauge (Million water level gauge, Yokogawa Co. Ltd., Tokyo, Japan). Discharge was calculated using Eq. (1). The amount of runoff (Q) was calculated as the daily discharge (D) divided by the drainage area, in mm day^{-1}.

(2) Groundwater level observation

Groundwater level was observed at the tower site (TS), located in the headwaters area of the O Thom I (OT1) sub-catchment (Fig. 1). The watershed measures 137 km^2 in area, ranging in elevation from 48 m to 273 m ASL. However, 90% of the total area is below 100 m altitude. A 60-m evapotranspiration observation tower has provided data used to observe the forest water cycle (Nobuhiro et al. 2007, Shimizu et al. 2007). Eleven wells are also located at this site, used for groundwater level observations. Wells numbered 1 to 8 were installed in 2003, and the other three (9-11) were installed in 2011. Well Nos. 1-5 are situated almost linearly along the river channel of a stream (Line-X), and well Nos. 6-11 lie

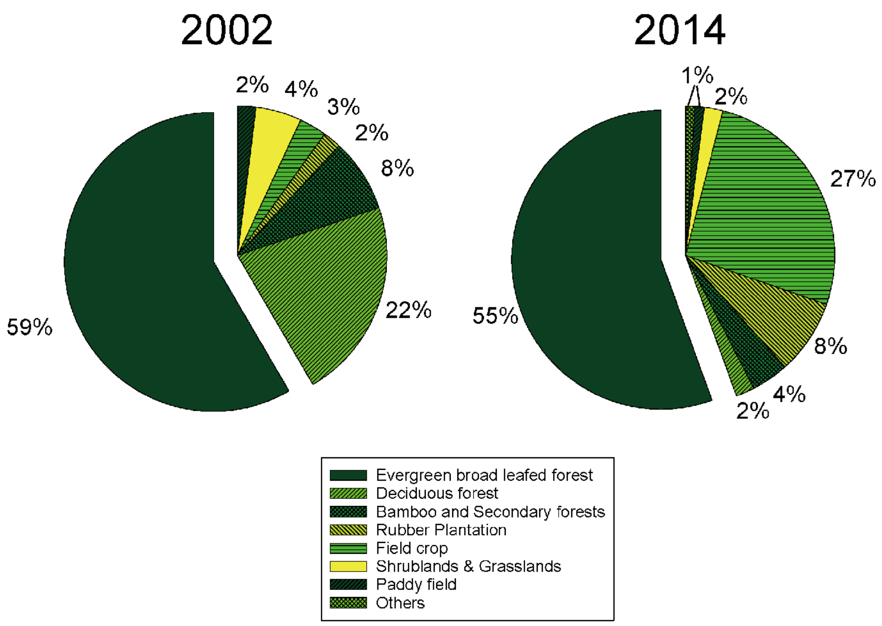

Fig. 2. Land use in the Stung Chinit (CT) watershed in 2002 and 2014, by percentage

perpendicular to the river channel (Line-Y) (Fig. 3). Well No. 6 is located in the rainfall interception plot, which is 30 m away from a stream that dries up during the dry season every year.

The well pipes are made of polyvinyl chloride, with small holes drilled into them, 4 m (well Nos. 1 to 8) and 5.5 m (well Nos. 9 to 11) in length. Many small holes at all depths of these wells are used as a strainer. They were inserted into the well holes with water-permeable bonded textile covering the buried parts of the pipes, protruding 0.4 m-0.5 m from the ground surface (Araki et al. 2008). This study site is located on mostly flat land with a soil-surface elevation of 1.3 m-2.2 m per 100 m horizontal distance (inclination: 0.7 m-1.3 m) (Araki et al. 2008). The groundwater level of the wells was measured manually once per day at 0900 since 1 August 2011, again using a buzzer-type water level gauge (Million water level gauge, Yokogawa Co. Ltd., Tokyo, Japan).

(3) Rainfall observations

Rainfall was observed at five locations—Bak Snar (BS), Dong Kda (DK), Kampub Ambel (KA), Kbal Domrey (KD), and Tower Site (TS)—and then measured using an RG-2M tipping bucket rain gauge and a HOBO event logger (Onset Computer Corp., Bourne, USA) at BS, DK, KA, and KD and an OW-34-BP tipping bucket rain gauge (Ota Keiki Seisakusho Co., Ltd., Tokyo, Japan) and a CR10X (Campbell Scientific, Inc., Logan, USA) at TS. These data were calculated as the amount of daily rainfall (mm day^{-1}). The rainfall at BS represents the watershed rainfall of CT (Kabeya et al. 2008). However, there were many missing data points at BS due to such rain gauge issues as overflow caused by blockage and data-logger failure during long-term observation.

To determine whether missing data can be substituted with data from nearby surrounding rain gauges, the relationship between rainfall levels at BS and those at other sites were investigated (Fig. 4) using annual rainfall data from five sites comprising a complete time series from 2003 to 2016. The TS and KD sites are 30 km and 50 km away from BS, respectively (Fig. 1), and both

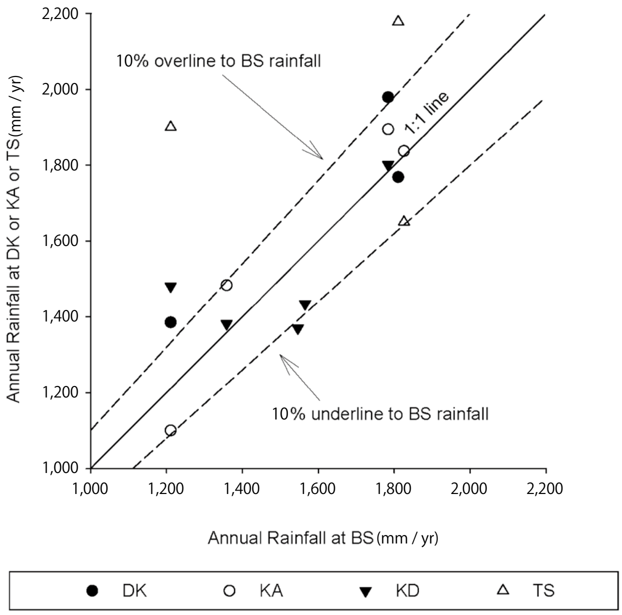

Fig. 4. Relationship between total annual rainfall at Bak Snar (BS) and the four other sites, Dong Kda (DK), Kamb Ambel (KA), Kbal Domrey (KD), and Tower Site (TS)

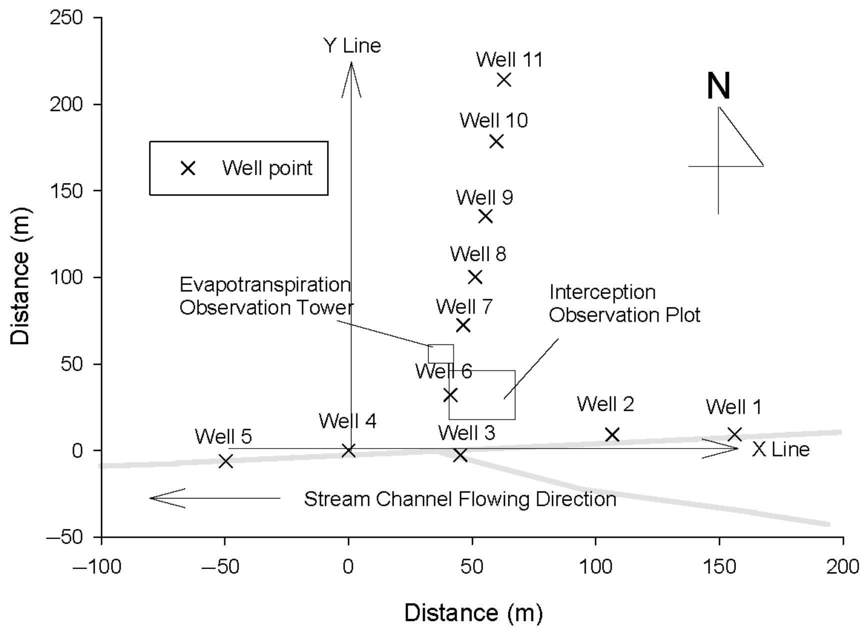

Fig. 3. Schematic showing the evapotranspiration observation tower and groundwater monitoring wells at the Tower Site (TS)

sites had a different pattern from that at BS (Fig. 4). The DK and KA sites are 10 km and 25 km away from BS, respectively, and have annual rainfall values that are generally distributed along the regression line with gradient 1 in relation to the BS values. Therefore, rainfall data from the DK and KA sites were used to represent watershed rainfall for the years of missing rainfall data at BS. Specifically, rainfall data from KA were used for 2007 and 2014-2016, and rainfall data from DK were used for 2011 and 2013.

(4) Identification of rainy and dry seasons

The beginning of the rainy season in the East Asian monsoon occurs around 17 May (Orgill 1967). There are several methods of determining the rainy season for each year. We used the method of Matsumoto (1997), defined as follows:

"The definition of the onset (withdrawal) of the summer rainy season is that of the first (last) pentad (5-days) when the mean pentad precipitation exceeds annual mean pentad precipitation [Pm = (Annual precipitation) / 73] in at least three consecutive pentads, following (before being) lower than it in more than three consecutive pentads. The middle date of this defined pentad is considered the onset or withdrawal date.

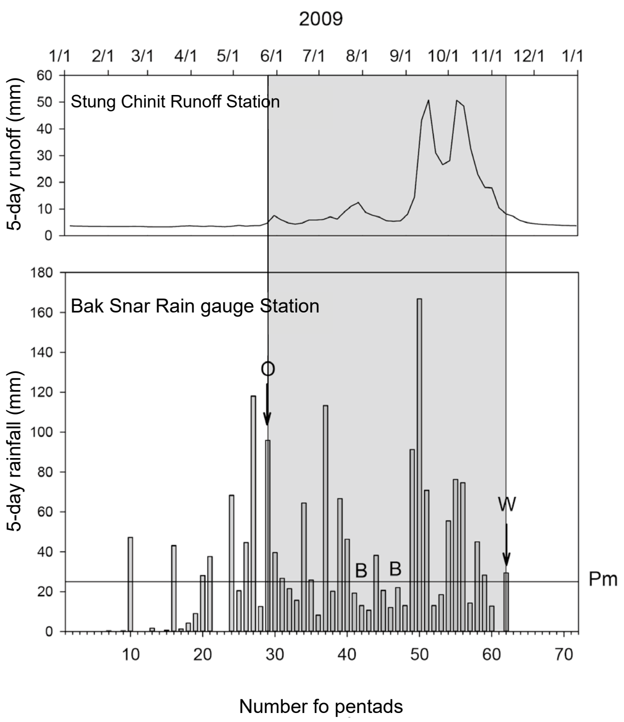

Fig. 5. Figure showing the rainy and dry seasons for Bak Snar (BS) rain gauge station in 2009, indicated by Matsumoto 1997's method

The runoff data of Stung Chinit (CT) watershed is also plotted. O, W, and B denote the onset, withdrawal, and break of the summer monsoon, respectively. Pm is annual mean pentad (5-day) precipitation.

Therefore, the threshold value for onset or withdrawal is different between station locations. This method is useful for regions such as Indochina where large differences in average precipitation are found due to orographic effects upon the mean monsoonal flow."

Figure 5 shows pentad (5-days) rainfall totals for the Bak Snar (BS) station in 2009. In this figure, onset and withdrawal of the summer rainy season are shown as marked "O (onset)" and "W (withdrawal)". The summer rainy season is divided into two rainy seasons by breaks (marked "B"), known as monsoon breaks, where the pentad precipitation is lower than Pm for more than three consecutive pentads. Takahashi & Yasunari (2006) noted that "the climatological monsoon break (same meaning as monsoon break) coincides with a drastic change in large-scale monsoon circulation in the seasonal march … (and it) divides the rainy season into the early monsoon and the later monsoon over the Indochina Peninsula." It is not clear how Matsumoto (1997) handled leap days. For our study, rainfall on leap days (29 February) was added to the 12th pentad (usually February 25 to March 1).

4. Southern Oscillation Index

Variations in the surface temperature of the Pacific Ocean are often associated with ENSO, which is the most important coupled ocean-atmosphere phenomenon causing global variability on an interannual timescale (Callaghan & Bonell 2005). The Southern Oscillation Index (SOI) can be used to represent ENSO activity, and is based on the difference in sea level pressure between Tahiti and Darwin. There are several methods of calculating the SOI, such as using the equation below as practiced by the Australian Government Bureau of Meteorology (AGBM).

$$SOI = 10 \left[P_{diff} - P_{diffav} \right] / SD\,(P_{diff}) \qquad (2)$$

where P_{diff} = (monthly average mean sea level pressure in Tahiti) − (monthly average mean sea level pressure in Darwin), P_{diffav} = long-term average of P_{diff} for the month in question, and SD(P_{diff}) = long-term standard deviation of P_{diff} for the month in question.

Using this equation, the SOI ranges from about −35 to about +35, and is usually given as a whole number. The SOI is usually computed on a monthly basis, with values over longer periods such as a year sometimes being reported. Suppiah (2004) reported long-term rainfall trends associated with recent climate change and the SOI. The SOI is associated with climate in the Asia-Oceania region that includes Thailand, India, Australia, and Japan (Liu et al. 1998, Shrestha & Kostaschuk 2005, Jin et al. 2005, Chandimala & Zubair 2007, Fu et al. 2013, Räsänen & Kummu 2013, Sun et al. 2014, Kabeya et al. 2016). In Southeast Asia and the Oceania region, an El Niño phase tends to result in high temperatures and water shortages, whereas the La Niña phase tends to bring substantial rainfall. In addition, the Australian Weather Bureau defines an El Niño/La Niña phase as being when the SOI is −7 and +7, respectively. However, the correlation between climate and the SOI varies by region.

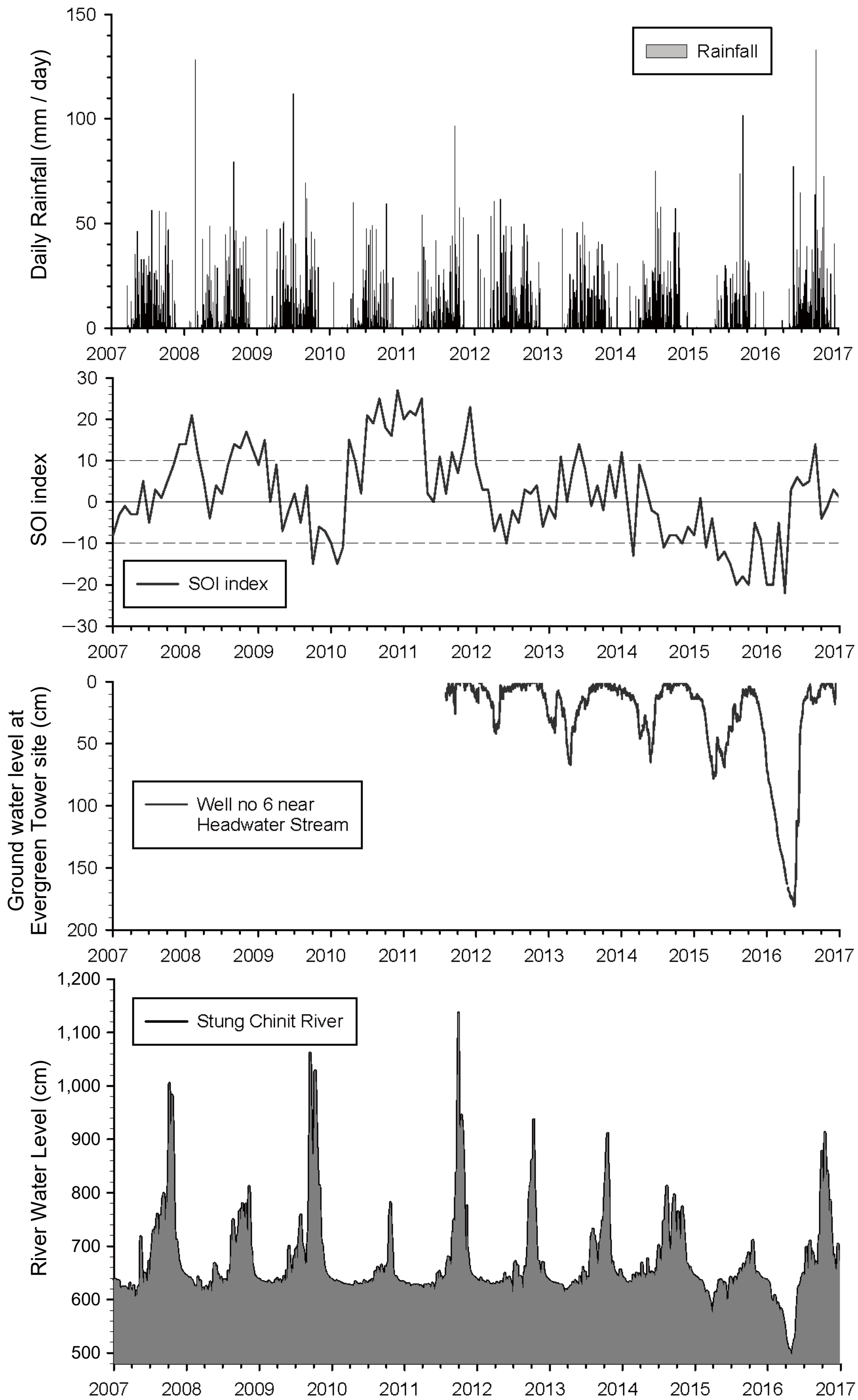

Fig. 6. Hydrological observations between 2007 and 2016 at the evergreen forest experimental watershed in Kampong Thom, Cambodia, showing daily rainfall (mm/day), groundwater level at TS (cm), and the water level of the Stung Chinit River (cm). SOI is also plotted.

We define an El Niño/La Niña phase using data from October-March inclusive, where the SOI is ±10.

Results

1. Results from long-term hydrological observations

Figure 6 shows the long-term hydrological observations for the 10 years from 2007 to 2016. Daily rainfall exceeded 100 mm/day in three cases: 24 February 2008 (128.2 mm/day), 1 July 2009 (112.0 mm/day), and 12 September 2016 (133.0 mm/day). However, many rainfall events had total daily amounts of less than 50 mm. Moreover, most rainfall events occurred between May and October, contributing to runoff (Fig. 6). Conversely, the lack of rainfall during the dry season resulted in marginal changes in the river water level. Seasonal variation in the river water level can be clearly observed, with an increase during the rainy season and a decrease during the dry season. The river water level at CT was 6 m or less for 26 days between 13 March and 7 April 2015, and 132 days between 18 January and 29 May 2016 during the dry season, corresponding to a strong El Niño event (Fig. 6).

Well No. 6 at TS was representative of the groundwater level, located at the headwaters of the OT1 sub-catchment, with the nearest stream being 30 m away

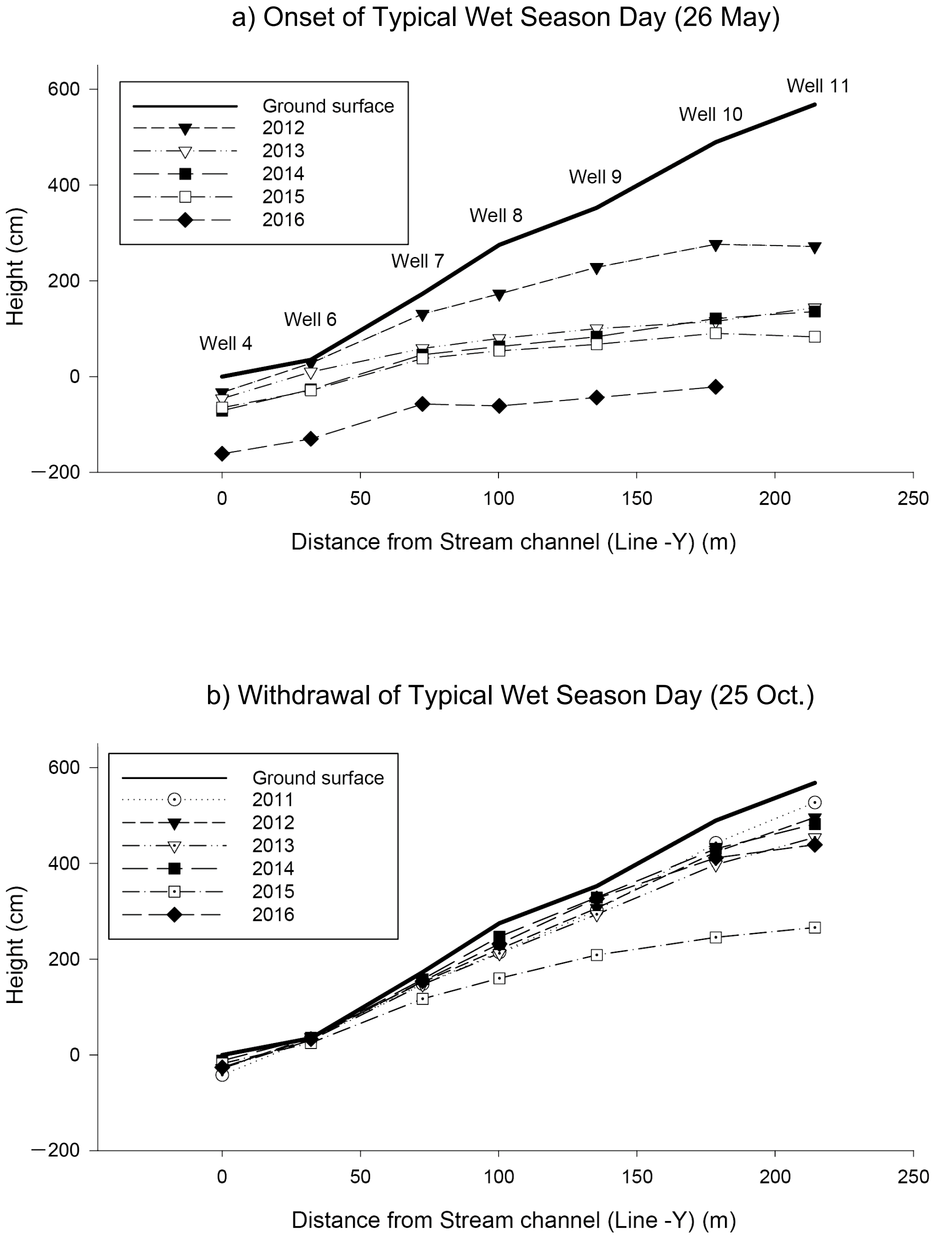

Fig. 7. Groundwater level at the onset and withdrawal of the rainy season at the Tower Site (TS) (line Y across a stream)

(Fig. 3). In 2012-2014, the groundwater level below the ground surface was 70 cm or less during the dry seasons, and reached the ground surface (0 cm) during the rainy seasons (Fig. 6). In 2015, the groundwater level below the surface reached as low as 82 cm, and then dropped to 190 cm in 2016. This behavior was also observed at well Nos. 8-11, although these wells are further away from the nearest stream. The SOI values during 2015-2016 were between −10 and −20 (Fig. 6), confirming the presence of a strong El Niño.

The maximum river water level at CT was 1,140 cm, recorded on 28 September 2011. At this time, the groundwater level at well No. 6 was at the ground surface. Between October 2010 and early 2011, the SOI was almost always greater than 20, which implies a strong La Niña phase. During this time, heavy rainfall occurred throughout Southeast Asia and serious flood damage occurred across Cambodia, Thailand, and Vietnam (MRC 2015).

2. Groundwater level at the onset and end of the rainy season

Figure 7 shows the groundwater levels for 26 May and 25 October for the Y lines across a stream (see Fig. 3). These two dates denote the average of the onset and withdrawal of the rainy season, respectively (see Section 4.). Well No. 6 had its minimum groundwater level at the onset of the rainy season, and its highest level at the withdrawal of the rainy season (Fig. 6). Although the figure was omitted, the groundwater level of the wells on the X line showed the same tendency in variation as those other wells (Nos. 4 & 6).

The groundwater levels of all wells were within 100 cm-150 cm of the ground surface at the withdrawal of all rainy seasons, apart from those on 25 October 2015 (Fig. 7b) when there was a strong El Niño event. As a result, the groundwater level beneath the ground surface was very low on 26 May 2016 after the following dry season (Fig. 7a). However, the usual groundwater level was restored at the end period of the rainy season on 25 October 2016 (Fig. 7b).

3. Annual water budget of the CT catchment

Table 1 lists the annual rainfall (P) of 1,625.8 mm, annual runoff (Q) of 468.0 mm, and annual loss (L) of 1,157.8 mm in the CT catchment. The annual rainfall

Table 1. Water balance observation result of the Stung Chinit (CT) watershed during 10 years (2007 to 2016)

Year	P [mm]	Q [mm]	L (= P − Q) [mm]
2007	1,679.6[#1]	632.1	1,047.5
2008	1,810.4	429.2	1,381.2
2009	1,825.6	691.9	1,133.7
2010	1,210.8	300.4	910.4
2011	1,666.4[#2]	583.6	1,082.8
2012	1,839.2	422.6	1,416.6
2013	1,607.0[#2]	445.9	1,161.1
2014	1,664.4[#1]	490.5	1,173.9
2015	1,110.8[#1]	266.4	844.4
2016	1,843.8[#1]	417.0	1,426.8
AVE	1,625.8	468.0	1,157.8
STD	247.2	129.0	191.7

#1: Rainfall data was used at the Kamb Ambel (KA) site.
#2: Rainfall data was used at the Dong Kda (DK) site.

Table 2. ENSO status and rain/dry season classification results of each year's ENSO status

Year	ENSO Status (SOI)	P (mm/y)	Onset of rainy season	Withdrawal of rainy season	Days of rainy season	Days of dry season	Days of monsoon break
2007	Neutral(±10)	1,679.6	4/26	10/17	175	190	
2008	La Niña (+21)	1,810.4	5/1	11/26	210	156	70
2009	La Niña (+15)	1,825.6	5/21	11/6	170	195	35
2010	El Niño (−16)	1,210.8	6/10	10/22	135	230	
2011	La Niña (+25)	1,666.4	6/10	10/17	130	235	
2012	La Niña (+23)	1,839.2	5/31	10/17	140	226	25
2013	Neutral (±10)	1,607	5/15	10/17	156	209	
2014	Neutral (±10)	1,664.4	6/10	10/27	140	225	
2015	El Niño (−14)	1,110.8	6/5	10/17	135	230	
2016	El Niño (−22)	1,843.8	6/15	10/22	130	236	15
		AVE	5/26	10/25	152	213	36
		STD	18	13	26	26	24

Light gray shade denotes a La Niña year; dark gray shade denotes an El Niño year.

exceeded 1,800 mm in 2008, 2009, 2012, and 2016. Conversely, the annual rainfall was less than 1,300 mm in 2010 and 2015. During the strong El Niño event in 2015, the annual rainfall was the lowest, with a value of 1,110.8 mm. The largest annual rainfall, with a value of 1,843.8 mm, occurred one year later in 2016.

4. Determining the rainy/dry season and ENSO status of each year

The rainy season of each year was determined using the method from Matsumoto (1997). This resulted in the average onset and withdrawal dates of the rainy season being 26 May and 25 October, respectively (Table 2). The rainy season was on average 152 days long, with a maximum (minimum) time period of 210 (130) days. The dry season was on average 213 days long, with a maximum (minimum) time period of 236 (156) days. Using these data, the ratio of the rainy-dry season length was approximately 2:3.

Monsoon breaks were observed in 4 of the 10 years, ranging in length from 15 to 70 days. Specifically, these breaks occurred three times in 2008, from 16-30 May, 15 June to 24 July, and 19 August 2 September; twice in 2009, from 20 July to 3 August, and 9-28 August; once in 2012 from 25 July to 18 August; and once in 2016 from 30 July to 13 August. Thus, the frequency ranged from 1 to 3 cases during these years. The breaks often occurred during late July to early August, with the centre of the period on 1 August.

The ENSO phase was determined for each year using the SOI values from October of the previous year to March of the year in question (Table 2). This resulted in three El Niños, four La Niñas, and three neutral cases. The years with a monsoon break also had a lot of precipitation, with totals above 1,800 mm per year. Among these years, 2016 marked an El Niño event, while 2008, 2009, and 2012 marked La Niña events. The years 2007, 2013, and 2014 were classified as neutral, and all had rainfall totals of approximately 1,600 mm per year, which was close to the average value of 1,625.8 mm per year for the 10-year study period.

Monsoon breaks did not occur in 2011, despite it being a La Niña year. In addition, the annual rainfall of 1,660 mm was close to the 10-year average value. However, flooding still occurred in September and October 2011 over a large area of the Indochinese Peninsula, specifically in Thailand, Cambodia, and Vietnam. The maximum river water level at CT was also observed during this period.

Discussion

1. Relationship between seasonal rainfall distribution and ENSO phase

Table 3 shows the seasonal distribution of precipitation throughout periods where an ENSO phase continued for two consecutive years, in order to investigate the relationship between ENSO and precipitation distribution. The rainy season was divided into two time periods (denoted w1 and w2), ending on

Table 3. Seasonal distribution of rainfall in the year when ENSO status continued for two years

	Rainfall of d1 (P_{d1}) mm	Rainfall of w1 (P_{w1}) mm	Rainfall of w2 (P_{w2}) mm	Rainfall of d2 (P_{d2}) mm	Ratio of P_{w2}/P_{w1}
a) La Niña state continued for two years					
2008	306.0	401.0	1,102.8	0.6	2.75
2009	437.4	575.8	812.4	0.0	1.41
2011	309.4	280.8	999.6	76.6	3.56
2012	548.2	510.4	659.4	121.2	1.29
b) Neutral state continued for two years					
2013	193.8	607.4	691.8	114.0	1.14
2014	269.6	584.4	791.4	19.0	1.35
c) El Niño state continued for two years					
2015	104.0	296.8	673.4	36.6	2.27
2016	247.4	422.2	953.4	220.8	2.26
				AVE	2.00

d1: dry season before the onset of rainy season
w1: rainy season before monsoon break
w2: rainy season after monsoon break
d2: dry season after rainy season

and starting after 1 August, respectively. The dry season rainfall was also split into two time periods (denoted d1 and d2), which comprise the first and second halves of the dry season, respectively.

The ratio of the first half to the second half of the rainy season (w1/w2) was, on average, 2.00. This ratio was a maximum of 3.56 in 2011. The ENSO phase was neutral in 2013 and 2014. The rainfall ratios (w2/w1) during both years were similar at 1.14 and 1.35, respectively.

The ENSO was in a La Niña phase for 2008-2009 and 2011-2012. The first year of each of these two-year periods had ratios (w2/w1) of 2.75 and 3.56, respectively. However, the second years had ratios of 1.41 and 1.29. The total rainfall in period d1 was 437.4 mm in 2009 and 548.2 mm in 2012, which are relatively large compared to the 2008 and 2011, the first years of the two-year La Niña events. Therefore, as the La Niña continued, an active rainfall pattern also continued into the dry season. And as a result, the ratio of the first half (w1) to the second half (w2) of the rainy season was small.

When the ENSO phase was in an El Niño phase, the second half of the rainy season (w2) had 953.4 mm over many rainfalls in 2016. The total rainfall during period d2 was 220.8 mm in 2016. Therefore, a lot of rainfall clearly occurred after the second half of the rainy season in 2016.

2. Relationship between ENSO phase and annual rainfall levels

We investigated the relationship between annual rainfall levels and ENSO phase. Three of the four La Niña years (2008-2010) had monsoon breaks and annual rainfall exceeding 1,800 mm (Table 2). In 2011, also a La Niña year, there were no monsoon breaks and the annual rainfall was 1,666.4 mm, although there was still flood damage from heavy rainfall in the Indochinese Peninsula, including Thailand and Cambodia. There appears to be a correlation between the years with large rainfall amounts over 1,800 mm and those in a La Niña phase. When the SOI indicated a neutral phase, the total annual precipitation was always close to the long-term average of 1,625.8 mm, and there were no monsoon breaks. For the El Niño years except 2016 (the year with an SOI of −20 or less), the average annual precipitation was 1,100 mm-1,200 mm. For the remaining years (2010 and 2015), the length of the rainy season was 22-27 days shorter than 152 days, on average.

Although 2016 was an El Niño year, it had monsoon breaks and large annual rainfall (of 1,843.8 mm). There was 953.4 mm of rainfall during the w2 period, comparable with the rainfall levels in w2 during the years 2008, 2009, 2011, and 2012. The latter four years were La Niña years (Table 3). The variability of the SOI during 2016 was studied more closely to investigate this finding. In April, it was −21, followed by an increase to +14 in September, and then a decrease to between ±10, indicating that it did not remain for long in the La Niña phase (Fig. 6). In other words, it is difficult to explain the increase in rainfall and large amounts of rainfall in the second half of the rainy season by using the SOI; therefore, it cannot be attributed to the ENSO phase.

Next, the Indian Ocean Dipole (IOD), a climate index in the Indian Ocean near Southeast Asia, was examined. A positive (negative) IOD is often associated with El Niño (La Niña) events, and a negative IOD corresponds to an increase in rainfall in Southeast Asia, Indochina, and Australia (AGBM 2012).

The strong El Niño of 2015/2016 broke down in the autumn of 2016, and a strong negative IOD influenced Australia’s climate from May to November (AGBM 2016), peaking in July with the largest negative values of the IOD index since reliable records were first kept in the 1960s. In addition, the Pacific Ocean exhibited a La Niña pattern during the second half of the year, with many climate indices approaching La Niña levels during spring. However, there was no La Niña event that year, and the tropical Pacific Ocean remained in an ENSO-neutral phase. The combination of a negative IOD and a La Niña pattern in the Pacific Ocean was associated with the wettest May to September on record for Australia.

This behavior was also reported by the Japan Agency for Marine-Earth Science and Technology (JAMSTEC) (2016) and Blunden & Arndt (2017). A negative IOD means that the ocean temperature in Indonesia is higher than normal, which can lead to an increase in convective activity with heavy rainfall in East Asia. Therefore, in combination with the La Niña pattern, this is what led to the increased precipitation in Australia, as well as the Indochinese Peninsula including Cambodia late in the year.

3. Monsoon breaks and seasonal rainfall distribution

Between 2007 and 2016, there were four years with monsoon breaks. Three of these years were in a La Niña phase, while the fourth was an El Niño year (Table 2), and no monsoon breaks occurred during ENSO-neutral years. The ratio of rainfall in the first half to the second half of the rainy season in the neutral years was approximately 1.2 (Table 3), indicating marginal differences in rainfall level in each half. However, for the La Niña and El Niño years, the second half of the rainy season had 2-3 times as much rainfall as in the first half.

The monsoon breaks occurred around 1 August, with an average length of 36 days, ranging between 15 and 70 days. Studies on rainfall in Thailand (Matsumoto 1997) showed that monsoon breaks begin at the end of June, whereas this study showed that such breaks begin around the end of July/early August in Cambodia.

Research on intra-seasonal rainfall in the Indochinese Peninsula has revealed the existence of two cycles: one with a period of 30-50 days (more evident at the coast), and the other with a period of 10-20 days (more evident inland) (Yokoi et al. 2007). The 10-20 day period of Active Day Ratio (ADR) is in good agreement with the variability of precipitation in southern Laos to central Vietnam. There are two peaks, in May-June and September-October, with a decrease in between in July and August (Yokoi et al. 2007), corresponding to the monsoon breaks. The peak in September-October is larger than the earlier peak, and thus in agreement with our finding that rainfall increased in the second half of the rainy season. Our research on the intra-seasonal variability of precipitation using long-term observations supports previous research on precipitation in this region.

A decrease in evapotranspiration was observed in 2015-2016, during the dry season that coincided with a strong El Niño (Shimizu et al. 2018). For other dry seasons where the bandpass method had successful measurements (2008-2009, 2011-2012, and 2013-2014), the same decrease was not observed (Shimizu et al. 2018). In the same 2015-2016 dry season, the groundwater level at well No. 11 was less than 5 m and approaching the bottom of the well, and the river water level at CT was also the minimum recorded, at less than 6 m. This implies that the water storage of the watershed decreased significantly during this period.

A dry evergreen forest can usually maintain active evapotranspiration during the dry season due to water absorption through its root system in deep soil. However, in severely dry seasons, the water content in the soil dramatically decreases, resulting in reduced transpiration activity, at approximately half the rate of that in a typical dry season. Should these conditions continue for a long period, plants may suffer irreversible physiological damage. However, there was 953.4 mm of rainfall in the second half of the rainy season in 2016 (Table 3). As a result, both river water and groundwater levels were restored to the same values as in the former period by the end of October (Figs. 6 and 7).

Ohnuki et al. (2008) estimated a soil water capacity of 1,100 mm in the dry evergreen forest near TS using soil depth measurements along with the effective porosity of soil. As some rainfall always contributes to direct runoff or evapotranspiration, not all rainfall turns into groundwater. However, the 953.4 mm of rainfall that occurred in the second half of the rainy season in 2016 was close to the soil water capacity; therefore, the watershed recovered almost immediately, without any apparent serious physiological damage.

Summary and conclusions

The relationship between the El Niño/Southern Oscillation (ENSO) and the water cycle of a forest watershed was studied using hydrological observations in a lowland, dry, evergreen forest catchment area of the lower Mekong River, Cambodia, from 2007-2016. The average annual rainfall, runoff, and loss were 1,625.8, 468.0, and 1,157.8 mm, respectively. The annual rainfall of neutral years, defined by the Southern Oscillation Index (SOI) as ranging between ±10, was close to 1,600 mm. The large amounts of annual rainfall (greater than 1,800 mm) were recorded in the La Niña years (SOI between +14 to +21) , and these years often had monsoon breaks during the rainy season. Aside from 2016, smaller amounts of annual rainfall (ranging between 1,100 mm and 1,200 mm) were recorded in the El Niño years (SOI < −10).

The rainy and dry seasons were classified following Matsumoto (1997). The onset of the rainy season was 26 May and the end was approximately 25 October. We found that the rainy season could be divided into two halves, split on 1 August, when monsoon breaks often occurred. Thus, we classified our data into four periods as follows: the dry season before the rainy season (d1), the first half of the rainy season (w1), the second half of the rainy season (w2), and the dry season after the rainy season (d2). These time periods effectively explain the hydrological data obtained from the study catchment, such as rainfall distribution and changes in groundwater level.

Variability in groundwater level at the end of the rainy season was smaller than that at the onset of the rainy season. This implies that water fills up the thick soil layers by the end of each year's rainy season. The vegetation in an evergreen forest maintains active transpiration during normal dry seasons due to water storage underground. However, during the dry season of 2015-2016 when there was a strong El Niño, the groundwater level by the end of the rainy season was extremely low. The river water level in the watershed had also decreased to below 6 m. However, 953.4 mm of rainfall occurred in the second half of the rainy season in 2016. This is approximately 85% of the soil water capacity estimated by Ohnuki et al. (2008) for the dry evergreen forest near TS. Both the groundwater and river water levels were restored to normal levels following this rainfall.

For the years in which monsoon breaks occurred, there were large rainfall totals, with more than 1,800 mm of annual precipitation. For the same years, the amount of rain during the second half of the rainy season (w2) was three times greater than that during the first half of the rainy season (w1). Therefore, the monsoon breaks may be correlated with the increased amount of rainfall in the second half of the rainy season. For future work, we will further examine the meteorological behavior to understand the role of monsoon breaks as rainfall drivers in this region.

Acknowledgements

We wish to thank Mr. Saing Satha and other staff members of the Forest and Wildlife Science Research Institute, Forestry Administration, Cambodia, for their filed support. Mr. Tatsuhiko Nobuhiro made significant contributions in organizing the evergreen forest experimental catchment in the early stages of observations. This study was partly funded by JSPS KAKENHI, (Grant Number 16K07799), and Kurita Water and Environment Foundation (Grant Numbers 15B008 and 16K002).

References

ADB (2012) *Cambodia: Stung Chinit irrigation and rural infrastructure project.* ADB, Manila.

ADB & UNEP (2004) *Greater Mekong Subregion Atlas of the environment*. ADB, Manila.

AGBM: *Southern Oscillation Index (SOI) since 1876*. http://www.bom.gov.au/climate/current/soi2.shtml.

AGBM (2012) *Record-breaking La Niña events: An analysis of the La Niña life cycle and the impacts and significance of the 2010-11 and 2011-12 La Niña events in Australia*. Melbourne, Australia.

AGBM (2016) *Annual climate statement 2016*. http://www.bom.gov.au/climate/current/annual/aus/2016.

Araki, M. et al. (2008) Seasonal fluctuation of groundwater in an evergreen forest, central Cambodia: Experiments and two-dimensional numerical analysis. *Paddy and Water Environ.*, **6**, 37-46.

Ashton, P. S. (1991) Toward a regional classification of the Humid Tropics of Asia. *Tropics*, **1**, 1-12.

Blunden, J. & Arndt, D. S. (2017) State of the Climate in 2016. *Bull. Amer. Meteor. Soc.*, **98**, Si-S277.

Callaghan, J. & Bonell, M. (2005) An overview of the meteorology and climatology of the humid tropics. *In* Forests, water and people in the humid tropics: Past, present and future hydrological research for integrated land and water management, eds. Bonell, M. & Bruijnzell, L. A., Cambridge University Press, Cambridge, pp. 158-193.

Chandimala, J. & Zubair, L. (2007) Predictability of stream flow and rainfall based on ENSO for water resources management in Sri Lanka. *J. Hydrol.*, **335**, 303-312.

Chappell, N. A. et al. (2007) Runoff processes in Southeast Asia: Role of soil, regolith, and rock type. *In* Forest environments in the Mekong River Basin, eds. Sawada, H. et al. Springer, Tokyo, pp. 3-23.

Fu, G. et al. (2013) Temporal variation of extreme rainfall events in China, 1961-2009. *J. Hydrol.*, **487**, 48-59.

Ito, E. et al. (2007) Use of ASTER optical indices to estimate spatial variation in tropical seasonal forests on the west bank of the Mekong River, Cambodia. *In* Forest environment in continental river basins, eds. Sawada, H. et al., Springer, Tokyo, pp. 232-240.

JAMSTEC (2016) *SINTEX-F Family Climate Prediction: Prediction from 1st Aug 2016*. http://www.jamstec.go.jp/aplinfo/sintexf/e/seasonal/outlook.html.

Jin, Y. -H. et al. (2005) Quantitative relationship between SOI and observed precipitation in Southern Korea and Japan by nonparametric approaches. *J. Hydrol.*, **301**, 54-65.

Ju, J. & Slingo, J. (1995) The Asian summer monsoon and ENSO. *Quarterly Journal of the Royal Meteorological Society,* **525**, 1133-1168.

Kabeya, N. et al. (2007) Stable isotope studies of rainfall and stream water in forest watersheds in Kampong Thom, Cambodia. *In* Forest Environments in the Mekong River Basin, eds. Sawada, H. et al., Springer, Tokyo, pp. 125-134.

Kabeya, N. et al. (2008) Preliminary study of flow regimes and stream water residence times in multi-scale forested watersheds of central Cambodia. *Paddy and Water Environ.*, **6**, 25-35.

Kabeya, N. et al. (2016) Quantification of the effect of forest harvesting versus climate on streamflow cycles and trends in an evergreen broadleaf catchment. *Hydrol. Sci. J.*, **61**, 1716-1727.

Liu, Z., Valdés, J. B. & Entekhabi, D. (1998) Merging and error analysis of regional hydrometeorologic anomaly forecasts conditioned on climate precursors. *Water Resour. Res.*, **34**, 1959-1969.

Malhi, Y. & Wright, J. (2004) Spatial patterns and recent trends in the climate of tropical rainforest regions. *Phil. Trans. R. Soc. Lond. Ser. B*, **359**, 311-329.

Matsumoto, J. (1997) Seasonal transition of summer rainy season over Indochina and adjacent monsoon region. *Adv. Atmos. Sci.*, **14**, 231-245.

MRC (2015) *Annual Mekong Flood Report 2011*. Phnom Penh, Cambodia.

Nobuhiro, T. et al. (2007) Year-round observation of evapotranspiration in an evergreen broadleaf forest in Cambodia. *In* Forest environments in the Mekong River Basin, eds. Sawada, H. et al., Springer, Tokyo, pp. 75-86.

Ohnuki, Y. et al. (2007) Apparent change in soil depth and soil hardness in forested areas in Kampong Thom Province, Cambodia. *In* Forest environment in continental river basins, eds. Sawada, H., et al., Springer, Tokyo, pp. 263-272.

Ohnuki, Y. et al. (2008) Distribution and characteristics of soil thickness and effects upon water storage in forested areas of Cambodia. *Hydrol. Process*, **22**, 1272-1280.

Orgill, M. (1967) *Some aspects of the onset of the summer monsoon over South East Asia.* Report to U.S. Army, Contract DA28-043-AMC-01303(E), Colorado State University.

Räsänen, T. & Kummu, M. (2013) Spatiotemporal influences of ENSO on precipitation and flood pulse in the Mekong river basin. *J. Hydrol.*, **476**, 154-168.

Rasmusson, E. M. & Carpenter, T. H. (1983) Variations in tropical sea surface temperatures and surface wind fields associated with the Southern Oscillation/ El Niño. *Mon. Wea. Rev.*, **110**, 354-384.

SCW (2006) *Atlas of Cambodia: National Poverty and Environment Maps.* Save Cambodia's Wildlife, Phnom Penh, Cambodia.

Shimizu, A. et al. (2007) Runoff characteristics and observations on evapotranspiration in forest watersheds, central Cambodia. *In* Forest environments in the Mekong River Basin, eds. Sawada, H. et al., Springer, Tokyo, pp. 135-146.

Shimizu, T. et al. (2018) Changing evapotranspiration under the effect of a strong El Niño in a natural tropical seasonal forest in Cambodia. *AGU 2018 fall meeting abstract*, H52E-08.

Shinomiya, Y. et al. (2007) Effect of soil water content on water storage capacity: Comparison between the forested areas in Cambodia and Japan. *In* Forest environments in the Mekong River Basin, eds. Sawada, H. et al. Springer, Tokyo, pp. 273-280.

Shrestha, A. & Kostaschuk, R. (2005) El Niño/Southern Oscillation (ENSO)-related variability in mean-monthly streamflow in Nepal. *J. Hydrol.*, **308**, 33-49.

Sun, X. et al. (2014) A general regional frequency analysis framework for quantifying local-scale climate effects: A case study of ENSO effects on Southeast Queensland rainfall. *J. Hydrol.*, **512**, 53-68.

Suppiah, R. (2004) Trends in the southern oscillation phenomenon and Australian rainfall and changes in their relationship. *Int. J. Climatol.*, **24**, 269-290.

Takahashi, H. G. & Yasunari, T. (2006) A climatological monsoon break in rainfall over Indochina-a singularity in the seasonal march of the Asian summer monsoon. *J. Climate*, **19**, 1545-1556.

Toriyama, J. et al. (2007) Acrisol sand adjacent soils under four different forests types in central Cambodia. *Pedologist*, **51**, 35-49.

Toriyama, J. et al. (2013) Soil physicochemical properties and moisture dynamics of a large soil profile in a tropical monsoon forest. *Geoderma*, **197**-**198**, 205-211.

Webster, P. J. & Yang, S. (1992) Monsoon and ENSO: Selectively interactive systems. *Quart. J. Roy. Meteor. Soc.*, **118**, 877-926.

Wikramanayaka, E. et al. (2002) *Terrestrial Ecoregions of the Indo-Pacific: A Conservation Assessment*. Island Press, Washington DC.

Yokoi, S. et al. (2007) Climatological characteristics of the intra-seasonal variation of precipitation over the Indochina Peninsula. *J. Climat.*, **20**, 5301- 5315.

Yoshifuji, N. et al. (2007) Factors affecting interannual variability in transpiration in a tropical seasonal forest in Northern Thailand: Growing season length and soil drought. *In* Forest environments in the Mekong River Basin, eds. Sawada, H. et al., Springer, Tokyo, pp. 56-66.

Zhang, Y. et al. (2002) Onset of the summer monsoon over the Indochina Peninsula: Climatology and interannual variations. *J. Climate*, **15**, 3206-3221.